Miner Deposita (2006) 41: 152–159
DOI 10.1007/s00126-005-0047-1

ARTICLE

Hua-Ying Liang · Ian H. Campbell · Charlotte Allen · Wei-Dong Sun · Cong-Qiang Liu · Heng-Xiang Yu · Ying-Wen Xie · Yu-Qiang Zhang

Zircon Ce^{4+}/Ce^{3+} ratios and ages for Yulong ore-bearing porphyries in eastern Tibet

Received: 18 February 2005 / Accepted: 21 December 2005 / Published online: 14 February 2006

Abstract Yulong ore-bearing porphyries, along the northwestern extension of the Red River–Ailao Shan fault system in eastern Tibet, consist of five porphyry deposits, containing a total of more than 8 million tons of copper resources. U–Th–Pb laser inductively coupled plasma mass spectrometry dating of zircon shows that the porphyries were emplaced in Early Tertiary (41.2–36.9 Ma), covering a period of ~4.3 Ma, with formation ages decreasing systematically from northwest to southeast. The start of porphyry magmatism coincided with the onset of transpressional movement along the Red River–Ailao Shan fault system, implying a close link between these two events. Age sequence in intrusions can be plausibly explained by assuming that a region of melting in the lower northwestern plate moved southeasternward along the Tuoba–Mangkang fault relative to the upper plate. Zircon grains from the Yulong ore-bearing porphyries have higher Ce^{4+}/Ce^{3+} than those from barren porphyries in the region. This suggests that the ore-bearing porphyries crystallized from a relatively oxidized magma, which has important implications for future ore exploration in the region and other Cu deposits in convergent margin environments in general.

Keywords Porphyry copper deposits · Geochronology · Zircon · Laser ablation ICP-MS · Continental subduction · Tibet

Editorial handling: R. King

H.-Y. Liang (✉) · Y.-W. Xie · Y.-Q. Zhang
Key Laboratory for Metallogenic Dynamics, Guangzhou Institute of Geochemistry, Chinese Academy of Sciences, Guangzhou 510640, China
e-mail: lianghy@gig.ac.cn

I. H. Campbell · C. Allen
Research School of Earth Sciences, Australian National University, Canberra ACT 0200, Australia

W.-D. Sun
Key Laboratory of Isotope Geochronology and Geochemistry, Guangzhou Institute of Geochemistry, Chinese Academy of Sciences, Guangzhou 510640, China

C.-Q. Liu
Institute of Geochemistry, Chinese Academy of Sciences, Guiyang 550002, China

H.-X. Yu
Guilin Institute of Technology, Guilin 541004, China

Introduction

Porphyry copper deposits occur mainly in subduction environments (Sillitoe 1972; Mitchell 1973; Griffiths and Godwin 1983; Sillitoe and Camus 1991; Camus and Dilles 2001), continental collision orogenic belts, and continental transform fault zones (Bowen and Gunatilaka 1977). In the last few decades, porphyry copper deposits in subduction-related environments have been extensively studied (Sillitoe 1972; Mitchell 1973; Griffiths and Godwin 1983; Sillitoe and Camus 1991; Camus and Dilles 2001). In contrast, porphyry copper deposits in continent collision orogenic belts and continental transform fault zones are much less studied; thus, their geneses are less understood (Hou et al. 2003). The Yulong copper belt is located in the northern rim of the Himalayan ore zone in eastern Tibet (Tang and Luo 1995). The belt is 300 km in length and formed along the northwestern extension of the Red River–Ailao Shan fault, a major sinistral fault system that formed during the collision of Indian and Eurasian continents (Fig. 1). This copper deposit belt consists of one giant copper deposit (Yulong), two large deposits (Duoxiasongduo and Malasongduo), and two medium-sized deposits (Mangzong and Zhanaga), as well as dozens of other porphyry mineralization occurrences (Ma 1990; Tang and Luo 1995; Hou et al. 2003), with a total length of about 300 km on the northern rim of the Himalayan ore-forming zone in eastern Tibet (Tang and Luo 1995). All the ore-bearing porphyries are similar in trace element and rare-earth element (REE) patterns and in Sr–Nd–Pb

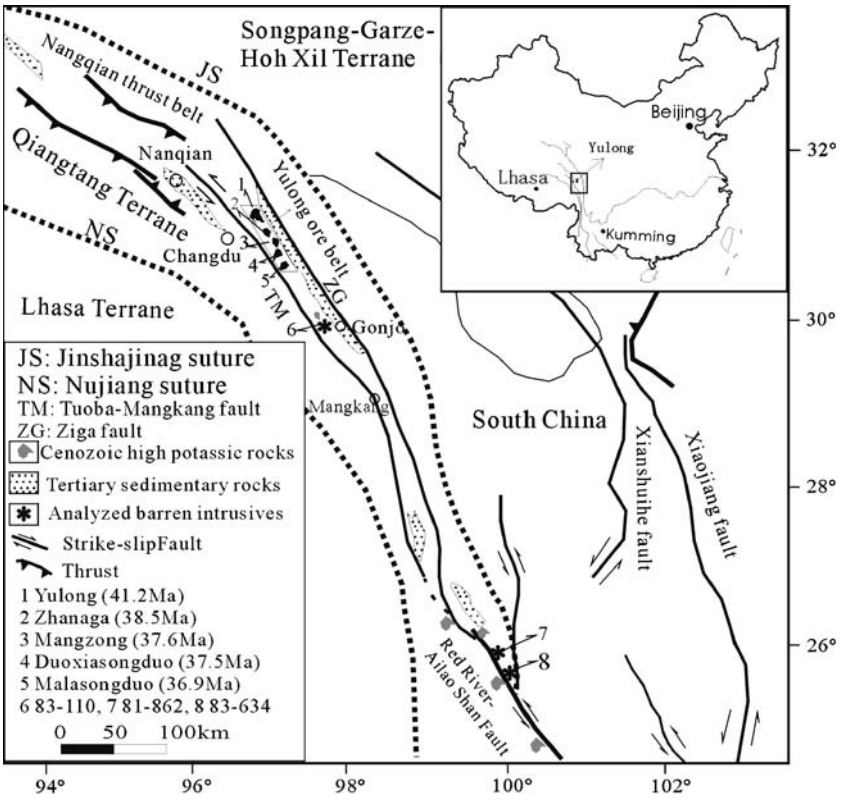

Fig. 1 Simplified geological map of the Yulong copper belt showing the location of the studied porphyries at the northern extension of the Red River–Ailao Shan fault system (modified after Yin and Harrison 2000; Hou et al. 2003; Tang and Luo 1995)

isotope compositions (Zhang et al. 1998; Hou et al. 2003; Tang and Luo 1995; Ma 1990), suggesting that they were formed in a similar tectonic setting and/or in analogous processes. The five big porphyries, which contain the highest Cu resource in the small domain, are examined in this paper.

Although the porphyries of the Yulong copper belt have been intensively studied, (Ma 1990; Rui et al. 1984; Tang and Luo 1995; Hou et al. 2003), their relationship with the tectonic environment in which they formed and with age of crystallization remains controversial. Ma (1990) and Rui et al. (1984) suggested that the Yulong porphyry copper deposit was formed in an island–arc environment. In contrast, Chen and Liao (1983) and Wang et al. (1995) argued that the porphyries of the Yulong copper belt formed in an intracontinental environment and are genetically related to an adjacent strike–slip fault zone. Hou et al. (2003) proposed that Yulong ore-bearing porphyries were developed in a Tertiary intracontinental convergent environment related to the collision of Indian and Eurasian continents and the associated uplift of the Tibetan Plateau.

The emplacement age of the ore-bearing porphyries is very important for understanding the tectonic environment in which the Yulong ore-bearing porphyries formed. One whole rock and 29 mineral K–Ar, 3 Rb–Sr, 1 zircon U–Pb, and 1 Ar–Ar ages have been published for these five ore-bearing porphyries of the Yulong copper belt (Ma 1990; Chen and Laio 1983; Liu et al. 1981; Zhang et al. 2000; Tang and Luo 1995). The isotopic ages for the Yulong, Zhanaga, Mangzong, Duoxiasongduo, and Malasongduo porphyries are in the ranges of 37.9–57.9, 33.9–40.0, 26.4–41.0, 27.8–51.9, and 32.4–49.2 Ma, respectively. Hou et al. (2003) therefore argued that the Yulong ore-bearing porphyries were emplaced in three periods (52, 40, and 33 Ma, respectively) based on these geochronological data. Given that the Yulong ore-bearing porphyries underwent potassium alteration, it is therefore highly probable that most of these K–Ar ages do not represent the formation age of the ore-bearing porphyries. Three Rb–Sr ages, two for Yulong (41.0 and 52.0 Ma) (Tang and Luo 1995; Ma 1990) and one for Duoxiasongduo (51.6 Ma) (Tang and Luo 1995) ore-bearing porphyries, define the oldest proposed emplacement age (Hou et al. 2003). Original data and uncertainties of Rb–Sr isotope compositions for the Duoxiasongduo porphyry have not been published; thus, it is difficult to evaluate the reliability of this age. Nonetheless, whole rock Rb–Sr isochron ages are usually considerably older than zircon U–Pb ages for intrusive rocks (Sun et al. 2002), and this Rb–Sr age is considerably older than published zircon isochron ages for the same sample [e.g., $^{235}U/^{204}Pb$ vs $^{207}Pb/^{204}Pb$ (40.9 Ma) and $^{238}U/^{204}Pb$ vs $^{206}Pb/^{204}Pb$ (33.7 Ma)] (Ma 1990). Therefore, the age of 51.6 Ma is likely to be too old. As for other Rb–Sr data, 41.0 Ma (Tang and Luo 1995) and 52.0 Ma (Ma 1990) for Yulong ore-bearing porphyries were model age and poor quality whole rock isochron age, respectively. The Rb–Sr isochron age for the Yulong ore-bearing porphyry was calculated by a low-quality fitting to ten samples. Nine of the samples have $^{87}Rb/^{87}Sr$ ratios of <1; the tenth sample has an $^{87}Rb/^{87}Sr$ ratio of 113. These nine samples with lower $^{87}Rb/^{87}Sr$ ratios clustered together and gave an "age" of 21.0±115 Ma, MSWD=44.5 when calculated using

ISOPLOT. The so-called isochron age (52.0 Ma) defined by ten samples was actually controlled by the sample with the highest $^{87}Rb/^{87}Sr$ ratio.

The zircon U–Pb isotope compositions from the Malasongduo ore-bearing porphyry give a lower intercept age of 31±140 Ma based on extrapolation from a discordant analysis, and age is clearly of poor quality.

The available data show that there is still a lot of controversy and uncertainty regarding the age of the five Yulong ore-bearing porphyries.

This study presents new U–Pb zircon ages for the five largest ore-bearing porphyries from the Yulong copper belt. We show that the zircon U–Pb ages of intrusions decrease systematically from northwest to southeast. We also present Ce^{4+}/Ce^{3+} ratios of zircon crystals from the ore-bearing porphyries and compare them with barren shoshonitic porphyries from elsewhere along the Red River–Ailao Shan fault system.

Geological setting

The Yulong copper belt is located in the Qiangtang terrane of the Himalayan–Tibetan orogen (Fig. 1), on the north rim of the Himalayan ore zone in eastern Tibet (Yin and Harrison 2000; Sengor and Natalin 1996; Tang and Luo 1995). The Himalayan copper zone is closely associated with a belt of Cenozoic shoshonitic intrusions that are aligned along the Red River–Ailao Shan fault zone and its northwestern extension (Zhang et al. 2000; Wang et al. 2001). The Yulong copper belt, covering a region of about 300 km long and 15–30 km wide, is bounded by a series of strike–slip faults, including the Tuobao–Mankang fault to the west and the Gonjo Tertiary basin and the Ziga fault to the east (Fig. 1) (Tang and Luo 1995). The five major porphyries, which contain the richest Cu resource, are located in a narrow, elongated domain, which is approximately 50 km long and 10 km wide and trends in a northwest–southeast direction (Tang and Luo 1995) (Fig. 1). The porphyries occur as small stocks, which intrude Triassic sandstone and limestone, and are characterized by epigenetic features such as explosive breccias. Individually, the ore-bearing porphyries have surface areas ranging from 0.1 to 0.7 km^2 (Tang and Luo 1995). A detailed geology of the Yulong copper belt is given in Hou et al. (2003) and Tang and Luo (1995).

The five largest ore-bearing porphyries can be distinguished by their texture and by variations in the proportion of phenocrysts that they contain. These ore-bearing porphyries typically comprise complex multiphase intrusions, dominated by two major intrusive stages (Zhang et al. 1998). In the Yulong ore-bearing porphyry (Fig. 1, no. 1), the two stages are an early quartz monzonite stage and a late syenogranite stage (Zhang et al. 1998). Both stages display massive porphyritic textures, with plagioclase, K-feldspar, hornblende, mica, and quartz phenocrysts set in a medium-grained phanerocrystalline matrix of similar mineralogy. The Yulong porphyry hosts a giant copper deposit with >6.5 million tons of copper at an average grade of 0.52% Cu and 0.15 million tons of molybdenum at an average grade of 0.028% Mo. The Zhanaga ore-bearing porphyry (Fig. 1, no. 2) is divided into an early monzogranite stage and a late syenogranite stage (Zhang et al. 1998). It is characterized by plagioclase, quartz, K-feldspar, minor mica, and rare hornblende phenocrysts set in a fine-grained phanerocrystalline matrix of similar mineralogy. The Zhanaga porphyry hosts more than 0.39 million tons of copper, with a copper content that typically varies between 0.2 and 0.4%. In the Mangzong and Duoxiasongduo ore-bearing porphyries (Fig. 1, nos. 3 and 4), the early stage is a monzogranite porphyry, whereas the late stage is an alkali–feldspar granite (Zhang et al. 1998). The Mangzong has plagioclase, K-feldspar, hornblende, mica, and minor quartz phenocrysts set in a phanerocrystal medium grain matrix. It contains more than 0.3 million tons of copper at an average grade of 0.3%. The Duoxiasongduo has K-feldspar, plagioclase, quartz, and mica phenocrysts set in an aphanitic matrix. The Duoxiasongduo porphyry hosts some 0.45 million tons of copper at an average grade of 0.36%. The two stages recognized in the Malasongduo porphyry (Fig. 1, no. 5) consist of an early alkali–feldspar granite stage and a late alkali–feldspar stage (Zhang et al. 1998). The Malasongduo porphyry has phenocrysts similar to those of the Duoxiasongduo porphyry. It hosts about 1 million tons of copper, with an average grade of 0.35%.

Analytical methods

Zircon separates were collected from relatively small rock specimens (~1 kg) from drill cores with the least alteration. Standard separation techniques were applied, including jaw splitting, crushing in swing mill, desliming in water, density separation in tetrabromoethane and methylene iodide, magnetic separation by isodynamic separator, and, finally, handpicking. Zircon grains were then mounted in epoxy and polished. Cathodoluminescent images and optical microscopy were used to ensure that the least fractured, inclusion-free zones in zircon were analyzed. Zircon analyses were performed in an inductively coupled plasma mass spectrometry (ICP-MS) laboratory at the Research School of Earth Sciences, the Australian National University, using the method described by Harris et al. (2004). Isotopes analyzed were: ^{29}Si, ^{31}P, ^{91}Zr, ^{177}Hf, ^{206}Pb, ^{207}Pb, ^{208}Pb, ^{232}Th, ^{235}U, ^{238}U, and six REEs. In brief, laser ablation was conducted by a pulsed ArF LambdaPhysik LPX 120IUV Excimer laser operated at a constant energy of 100 mJ, with a repetition rate of 5 Hz and a spot of 29 μm in diameter. The ablated material was carried by He–Ar gas from a custom-designed sample cell and a flow homogenizer to an Agilent 7500s ICP-MS. Samples were ablated alongside zircon and glass standards in rotation, as follows: Temora zircon standard (Black et al. 2003; two analyses), Los Picos in-house zircon standard (one analysis), NIST 610 standard glass (Pearce et al. 1997; Hinton 1999) (one analysis), and unknown zircons (four populations with two analyses of each).

Beyond uncertainties in individual ablation, an additional component of uncertainty (~1.5%) based on replicated analyses of Temora (the primary zircon standard) was added in quadrature for each analysis. For the in-house standard 98-521, the resulting MSWDs on the bulk population were generally 1.0–1.8, consistent with these zircon grains being from a single age population. Data with observed-errors/expected-errors ratios of >2 or those with <95% discordancy in $^{207}Pb/^{235}U$ or $^{208}Pb/^{232}Th$ with $^{206}Pb/^{238}U$ at the 1σ level were rejected in the final age determination.

More than 25 zircon grains were analyzed per rock sample, making it possible to process the data using statistical methods in the final data calculation. Zircon grains often display inheritance or lead loss, which complicates the interpretation of the U–Pb age of a given sample. To identify the core in zircon grains and grains that have undergone Pb loss, all data sets were processed using cumulative probability plots. Cumulative probability plots have a nonlinear scale on the *x*-axis that is calibrated to represent a normal distribution as a straight line of a positive slope. Old U–Pb outliers (lying above the projection of the straight line) were interpreted to be inherited cores in zircon grains, and young U–Pb outliners (lying below the line) were interpreted to have suffered Pb loss. The U–Pb ages of the main population are obtained by removing grains from both ends of the main population until the tails have a gradient equal to or lower than the main population at both ends of the spectrum. Outliers were omitted using these criteria, and a mean and MSWD were calculated for the remaining U–Pb data. The U–Pb age determined in this way was interpreted to be the cooling or crystallization age of the intrusion.

Zircon Ce^{4+}/Ce^{3+} and Eu/Eu* were calculated using the data collected during the same analysis interval as used for U–Pb dating. The theory for calculating these ratios has been reported in Ballard et al. (2002).

Results

Rock samples for the early and late intrusive stages from the ore-bearing porphyries were dated to determine whether there is a detectable age difference between the two stages. Weighted mean zircon U–Th–Pb ages for both the first and last stages of each intrusion are listed in

Table 1 Summary of excimer laser ablation ICP-MS U–Pb zircon ages (in Ma) for the Yulong ore-bearing porphyries

Porphyries	Samples	Number of analyses	Number of excluded	Bulk age[a] (Ma) ±2σ MSWD	Number of main population grains	Main population age[a] (Ma) ±2σ MSWD	Number of inherited grains	Inheritance age[a] (Ma)	Number of Pb loss grains	Pb loss age[a] (Ma)
Yulong	Early (A)	47	4	41.3±0.3 2.34	36	41.3±0.3 0.92	2	43–44	5	<40
	Late (B)	42	3	40.9±0.4 4.13	30	41.2±0.3 1.24	2	43–45	7	<39.5
	A + B	89	7	41.0±0.3 3.20	5	41.2±0.2 1.06	4	43–45	12	<40
Zhanaga	Early (A)	31	1	38.5±0.2 1.12	30	38.5±0.2 1.12	0		0	
	Late (B)	29	1	38.5±0.2 1.08	28	38.5±0.2 1.08	0		0	
	A + B	60	2	38.5±0.2 1.04	58	38.5±0.2 1.04	0		0	
Mangzong		29	4	37.5±0.3 1.80	24	37.6±0.2 1.40	0		1	35.3
Duoxiasongduo	Early (A)	26	2	37.2±0.4 2.82	21	37.4±0.3 1.84	0		3	<36.2
	Late (B)	30	3	37.5±0.3 2.75	21	37.6±0.2 0.99	3	>39	3	<36.5
	A + B	56	5	37.4±0.3 2.88	43	37.5±0.2 1.49	3	>39	5	<36.2
Malasongduo	Early (A)	25	4	37.1±0.6 3.30	18	36.8±0.3 1.15	3	>38.9	0	
	Late (B)	31	7	37.1±0.6 6.31	19	36.9±0.3 1.38	3	>39	2	<35.2
	A + B	56	11	37.1±0.4 4.80	38	36.9±0.4 1.25	6	>38.9	2	<35.2

[a] ^{208}Pb correct

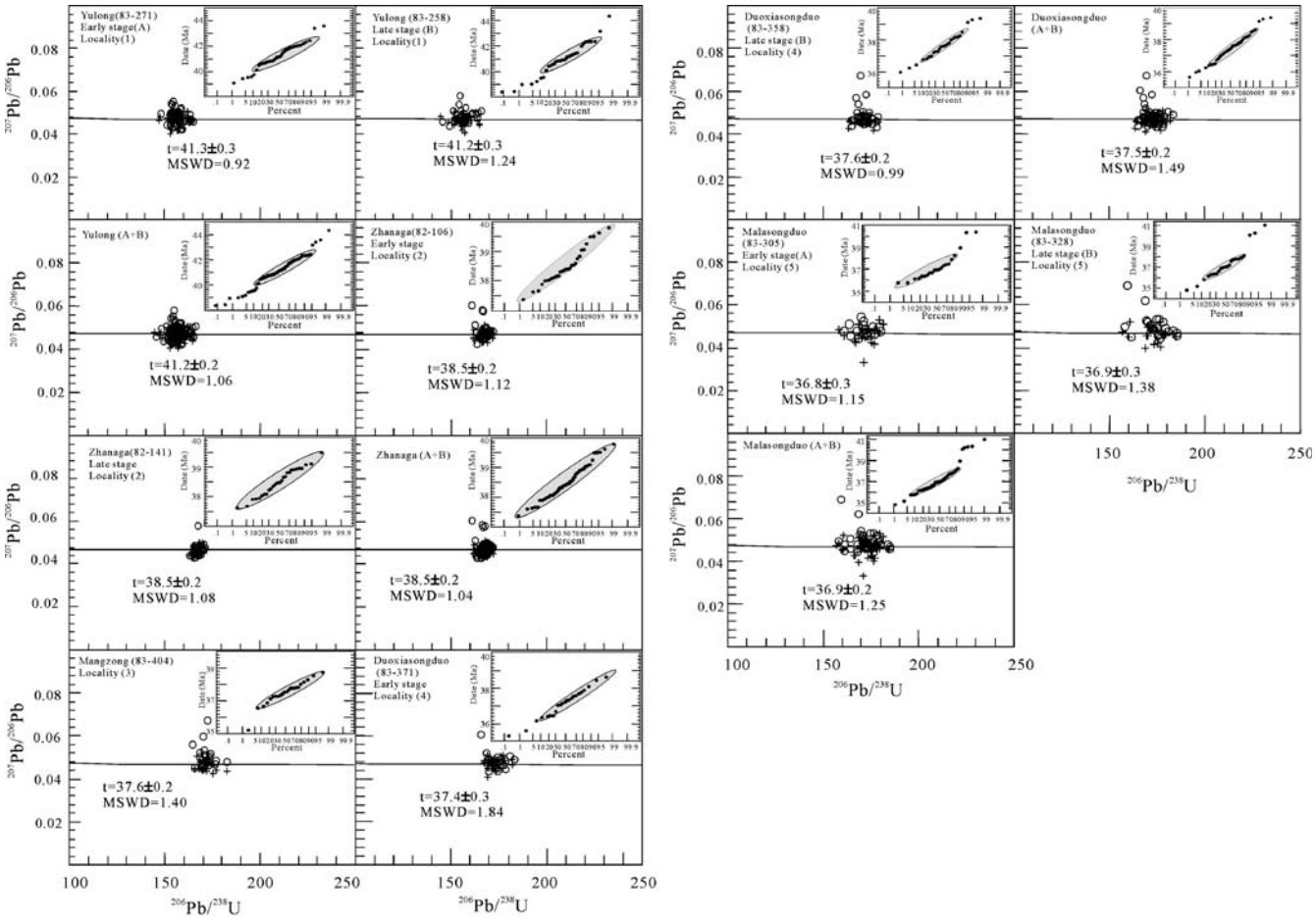

Fig. 2 Concordia plots showing the zircon U–Th–Pb analyses of the Yulong ore-bearing porphyries. The data in the plots have been culled of excessively scattered and discordant analyses following the criteria described in the text. *O* Before ^{208}Pb correction for common Pb; + after ^{208}Pb correction for common Pb. The *insets* are probability plots

Table 1, and the concordia and probability plots are shown in Fig. 2. Samples from the early and late intrusive stages, collected from the same porphyries, give U–Pb ages that agree well within analytical error (±2σ), suggesting that the two stages as well as multiphase intrusions form part of a continuum of a single magmatic event. Taking this into consideration, stage 1 and stage 2 data were pooled together to obtain more precise ages for the different porphyries. The pooled ages for the ore-bearing porphyries are Yulong (41.2±0.2 Ma, MSWD=1.06), Zhanaga (38.5±0.2 Ma, MSWD=1.04), Mangzone (37.6±0.2 Ma, MSWD=1.40), Duoxiasongduo (37.5±0.2 Ma, MSWD=1.49), and Malasongduo (36.9± 0.4 Ma, MSWD=1.25).

The Ce^{4+}/Ce^{3+} and Eu/Eu* ratios were determined for all of the dated zircon grains, primarily as a measure of the oxidation state of the magma (Ballard et al. 2002), but they also are temperature-dependent. Calculated zircon Ce^{4+}/Ce^{3+} ratios of the Yulong ore-bearing porphyries, and related barren shoshonitic porphyries from elsewhere along the Red River–Ailao Shan fault system (Fig. 1) with zircon ages varying from 34.5 to 38.5 Ma are plotted in Fig. 3 and listed in Table 2. The zircon Ce^{4+}/Ce^{3+} ratios of the Yulong ore-bearing porphyries vary greatly with high average ratios: Yulong, range 5–756, with an average of 204±37 (2σ); Zhanaga, range 26–729, with an average of 334±72 (2σ); Mangzong, range 18–1,230, with an average of 201±104 (2σ); Duoxiasongduo, range 10–1,314, with an average of 250±73 (2σ); Malasongduo, 17–1,304, with an

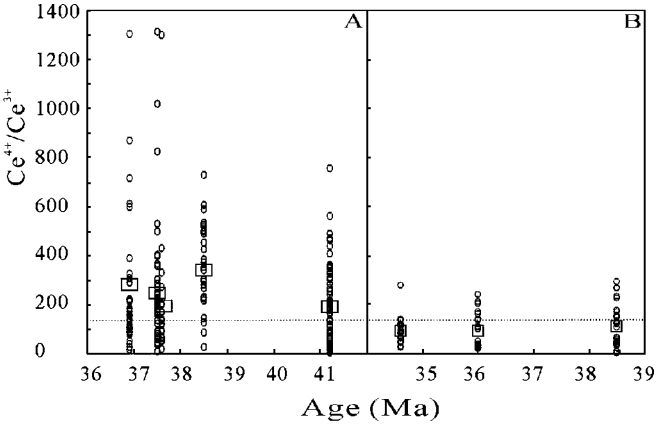

Fig. 3 Zircon Ce^{4+}/Ce^{3+} ratios of the Yulong ore-bearing porphyries (**a**) and barren porphyries (**b**). The *dash line* represents the boundary between the ore-bearing porphyries and the barren porphyries

Table 2 Zircon Ce^{4+}/Ce^{3+} ratios from the ore-bearing porphyries and barren porphyries in eastern Tibet

Porphyries		Ages (Ma)	Number analyzed	Range of Ce^{4+}/Ce^{3+} ratio	Average $\pm 2\sigma$
Ore-bearing	Yulong	41.2±0.2	77	5–756	204±37
	Zhanaga	38.5±0.2	47	26–729	334±72
	Mangzong	37.6±0.2	24	18–1,230	201±104
	Duoxiasongduo	37.5±0.2	47	10–1,314	250±73
	Malasongduo	36.9±0.4	38	17–1,304	258±94
Barren	83-810	38.5±0.2	27	3–295	112±34
	81-862	34.3±0.4	18	24–281	93±28
	83-634	36.0±0.4	23	23–244	93±30

average of 258±94 (2σ). The zircons from barren porphyries in eastern Tibet, on the other hand, have smaller variations of Ce^{4+}/Ce^{3+} ratios and lower average ratios (<120) (Fig. 3). Eu anomalies are not distinct between ore-bearing and barren groups.

Discussion

Geochronology

The emplacement ages for the porphyries in the Yulong copper belt vary between 41.2 and 36.9 Ma, which give a lifespan for shoshonitic magmatic activity in the Yulong copper belt of 4.3 Ma. This protracted period of intrusive activity in the Yulong District is similar to that of the Los Picos–Fortuna/Pajonal–El Abra complex (5.5 Ma) associated with the El Abra porphyry copper deposit in northern Chile (Ballard 2001). The long lifespan associated with giant porphyry copper deposits in different tectonic settings suggests that a protracted period of intrusive activity may favor the formation of these giant deposits.

The age of the porphyries decreases systematically from Yulong in the northwest to Malasongduo in the southeast (Fig. 1). The time gap between the Yulong (41.2±0.2 Ma) and the Zhanaga (38.5±0.2 Ma) porphyries is 2.7±0.2 Myr, and that between the Zhanaga and the Mangzong (37.6±0.2 Ma) porphyries is 0.9±0.2 Myr. The Duoxiasongduo porphyry (37.5±0.2 Ma) is almost of the same age as the Mangzong porphyry (37.6±0.2 Ma), and the time gap between the Duoxiasongduo and the Malasongduo (36.9±0.4 Ma) porphyries is ca. 0.5±0.4 Myr. The Yulong ore-bearing porphyries therefore received at least four separate pulses of magmatism and associated ore-forming hydrothermal activity between 41.2±0.2 and 36.9±0.4 Ma.

Tectonic model for the Yulong copper ore belt

The zircon U–Pb ages of the Yulong ore-bearing porphyries range from 41.2 to 36.9 Ma. During the Eocene–Oligocene, eastern Tibet underwent a period of contraction and transpression, caused by the collision of Indian and Eurasian continents (Wang et al. 2001; Wang and Burchfiel 1997; Pan et al. 1990; Ratschbacher et al. 1996). The movement along the Red River–Ailao Shan fault system was sinistral during the Tertiary and was transpressional between about 42 and 24 Ma (Ratschbacher et al. 1996; Wang and Burchfiel 1997). The correlation between the onset of transpressional tectonics in the region and the start of shoshonitic magmatism is unlikely to be coincidental. One plausible model is that the compressional component of the overall movement along the Red River–Ailao Shan and Batang–Lijiang faults had a significant vertical component that pushed one of the adjacent continental blocks into the upper mantle. The fault, which was locally responsible for this vertical movement in the Yulong copper belt, was probably the Tuoba–Mangkang fault (Fig. 1, TM). The tectonic model presented here for the origin of the shoshonitic porphyries is similar to that proposed by Wang et al. (2001) for the Cenozoic high potassic igneous activities along the Red River–Ailao Shear fault. The systematic northwest to southeast age progression of the Yulong porphyries is compatible with the context of the above tectonic model. If the source of heat—and therefore magmatism—is assumed to be a fixed point, then the systematic age progression of intrusions can be explained if the lower northwestern plate moved southeast along the

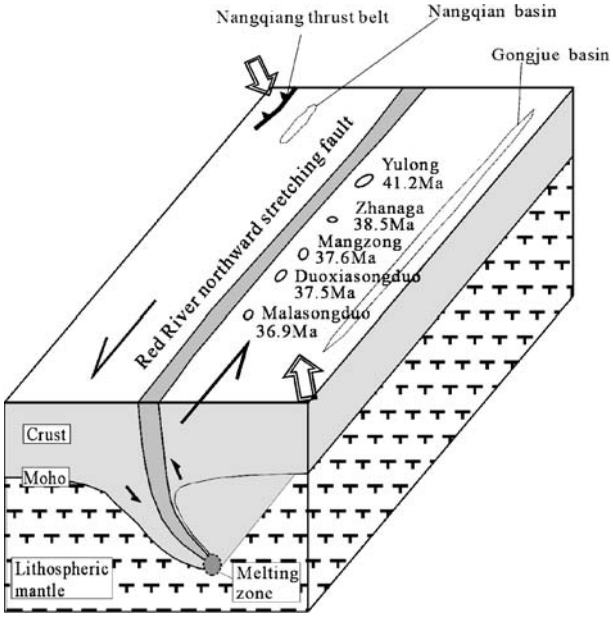

Fig. 4 Schematic tectonic model for the Yulong porphyry copper ore belt

Tuoba–Mangkang fault, over a local downthrusted region of the lower continental crust in the lower plate, at a rate of 1.2 cm/year (Fig. 4). The sinistral movement of the Tuoba–Mangkang fault (Fig. 1, TM) is in the direction predicted by this hypothesis and is consistent with what is known about the relative motion of theses two plates. This model, however, is not without problems because the assumption of a fixed point for the source of heat and magmatism is problematic. However, it does suggest that magmatism originated from a restricted zone within the lower plate; otherwise, the calculated relative movement between the plates would not be consistent with the expected movement. The Nangqian thrust and basin northwest of the Yulong porphyries and the Gonjo basin east of the Yulong porphyries may represent the foreland basins formed by the transpressional phase of the Red River–Ailao Shan and Batang–Lijiang fault systems (Figs. 1 and 4).

Zircon Ce^{4+}/Ce^{3+} ratio and its application

Zircons from the Yulong ore-bearing porphyries have higher mean Ce^{4+}/Ce^{3+} and much higher maximum values than those from barren porphyries from the same region (Fig. 3). A line has been drawn at a Ce^{4+}/Ce^{3+} ratio of 120 in Fig. 3 to divide the ore-bearing porphyries and the barren porphyries. This division can potentially be used in ore exploration in the region of the Red River–Ailao Shan Fault zone. This is different from the value of 300 used by Ballard et al. (2002) for the Chuquicamata–El Abra area in northern Chile. Nonetheless, this study supports the conclusion of Ballard et al. (2002) that Ce^{4+}/Ce^{3+} ratios can be used to separate ore-bearing intrusions from barren porphyries, but suggest that the Ce^{4+}/Ce^{3+} ratio that separates them may vary from district to district.

Regional differences in the Ce^{4+}/Ce^{3+} ratio could stem from the overall magma type and inherent magma temperatures. Higher Ce^{4+}/Ce^{3+} ratios are favored by higher oxygen fugacity and by lower magmatic temperature. The Yulong shoshonitic magmas give an average Zr saturation temperature of 825±29°C, using the method of Watson and Harrison (1983). In comparison, ore-bearing calc-alkaline rocks with similar silica contents from the Chucquicamata–El Abra area give average temperatures of 786±16°C. Hotter temperatures mitigate the oxygen fugacity effect of greater anomaly and may explain the differences of the magnitude of the Ce anomaly value that divides barren from ore-bearing rocks in the two regions.

Often within suites of related intrusions in an ore district, some are ore-bearing whereas others are not. The Ce^{4+}/Ce^{3+} ratio of zircon crystals provides a tool to distinguish the ore-bearing intrusions from barren ones, which may be useful for future ore exploration.

Implications for the genesis of copper mineralization

The zircon Ce^{4+}/Ce^{3+} ratio is controlled mainly by the oxygen fugacity of the magma and, to a lesser extent, by the temperature of crystallization (Ballard et al. 2002). Zircon grains from ore-bearing porphyries have higher Ce^{4+}/Ce^{3+} ratios than those of barren porphyries, suggesting that the ore-bearing porphyries formed from more oxidized and/or cooler melts. Empirical associations suggest that oxygen fugacity is the dominant effect given that the link between oxidized felsic magmas and mineralization is well known (Candela 1992; Blevin and Chappell 1992; Hedenquist and Lowenstern 1994; Ballard et al. 2002; Mungall 2002; Sun et al. 2004). The oxygen fugacity of a magma controls the oxidation state of sulfur in a melt: at low oxygen fugacity, sulfur in the magma exists mainly as S^{2-}, whereas at high oxygen fugacity, it exists mainly as SO or SO_2. The transition of S^{2-} to SO or SO_2 may prevent the saturation of an immiscible sulfide phase that scavenges Cu from a fractionating melt (Sun et al. 2004). Copper in a magma with high oxygen fugacity will then become enriched during differentiation and partition into a magmatic–hydrothermal fluid (Cline and Bodnar 1991; Pasteris 1996; Urich et al. 1999; Ballard et al. 2002; Sun et al. 2004).

If the shoshonitic porphyries of the Yulong copper belt are due to melting of the lower crust that has been pushed into the upper mantle along a major transpressional fault, then the high oxidation state of the magmas is inherited from the lower crust.

Conclusion

1. The shoshonitic porphyries of the Yulong copper belt formed between 41.2 and 36.9 Ma and show a systematic age progression from northwest to southeast. The lifespan of magmatic activities associated with the Yulong giant porphyry copper deposit is 4.3±0.4 Ma. The Yulong ore-bearing porphyries underwent four pulses of magmatic and related magmatic–hydrothermal events.
2. The age progression in the Yulong porphyries can be explained by the northwestern plate moving over a local region that pushed the continental crust down into the mantle.
3. The ore-bearing porphyries of the Yulong area have higher zircon Ce^{4+}/Ce^{3+} ratios than barren shoshonites from the same region, implying that the Yulong porphyries have crystallized from more oxidized magmas than the barren magmas. This has valuable implication for future exploration.

Acknowledgements We thank the Tibet Geological Survey for its help in our field work. Liang Huaying thanks the Chinese Academy of Sciences for supporting his visit to the Research School of Earth Sciences, Australian National University. The first author would like to thank the Research School of Earth Sciences for access to the excimer laser ablation ICP-MS and mineral separation facilities. This work was cosupported by the Chinese NSF (40472049 and 48972035), the Chinese National Key Project for Basic Research (G1999043203), and the Chinese Academy of Sciences Key Project (kzcx2-sw-117 and GIGCX-04-03). Victor Maksaev, Osvaldo Rabbia, Larry Meinert, and Rob King are thanked for greatly improving the manuscript through their thoughtful and thorough reviews.

References

Ballard JR (2001) A comparatives study between the geochemistry of ore-bearing and barren calc-alkaline intrusions. Unpublished PhD thesis, Australian National University, pp 1–250

Ballard JR, Palin JM, Campbell IH (2002) Relative oxidation states of magmas inferred from Ce(IV)/Ce(III) in zircon: application to porphyry copper deposits of northern Chile. Contrib Mineral Petrol 144:347–364

Black LP, Kamo SL, Allen CM, Aleiniloff JN, Davis DW, Korsch RJ, Foudoulis C (2003) TEMORA 1: a new zircon standard for Phanerozoic U–Pb geochronology. Chem Geol 200:155–170

Blevin PL, Chappell BW (1992) The role of magma sources, oxidation states and fractionation in determining the granite metallogeny of eastern Australia. Trans R Soc Edinb Earth Sci 83:305–316

Bowen R, Gunatilaka A (1977) Copper: its geology and economics. Applied Science Publishers, Ltd., London, pp 1–150

Camus F, Dilles JH (2001) A special issue devoted to porphyry copper deposits of northern Chile. Econ Geol 96:233–237

Candela PA (1992) Controls on ore metal ratios in granite-related ore systems: an experimental and computational approach. Trans R Soc Edinb Earth Sci 83:317–326

Chen FZ, Liao, GX (1983) The geology and major mineral resources in the Changdu area: contribution to the geology of the Qinghai–Tibet Plateau, vol 13. Geological Publishing House, Beijing, pp 1–168 (in Chinese with English abstract)

Cline JS, Bodnar RJ (1991) Can economic porphyry copper mineralization be generated by a typical calc-alkaline melt? J Geophys Res 96:8113–8126

Griffiths JR, Godwin CI (1983) Metallogeny and tectonics of porphyry copper–molybdenum deposits in British Columbia. Can Earth Sci 20:1000–1018

Harris AC, Allen CM, Bryan SE, Campbell IH, Holcombe RJ, Palin MJ (2004) ELA-ICP-MS U–Pb zircon geochronology of regional volcanism hosting the Bajo de la Alumbrera Cu–Au deposit: implications for porphyry-related mineralization. Miner Depos 39:46–67

Hedenquist JW, Lowenstern JB (1994) The role of magmas in the formation of hydrothermal ore deposits. Nature 370:519–527

Hinton RW (1999) NIST SRM 610, 611 and SRM 612, 613 multi-element glasses: constraints from element abundance ratios measured by microprobe techniques. Geostand Newsl 23:197–207

Hou ZQ, Ma HW, Zaw K, Zhang YQ, Wang MJ, Wang Z, Pan GT, Tang RL (2003) The Himalayan Yulong porphyry copper belt: product of large-scale strike–slip faulting in eastern Tibet. Econ Geol 98:125–145

Liu RM, Zhao DH, Huang XR (1981) Discussion on isotopic ages of acid intrusions in the eastern Tibet. Geol Rev 27:323–332 (in Chinese with English abstract)

Ma HW (1990) Granitoid and mineralization of the Yulong porphyry copper belt in eastern Tibet. China University of Geosciences Press, Wuhan, pp 1–158 (in Chinese with English abstract)

Mitchell AHG (1973) Metallogenic belts and angle of dip of Benioff zones. Nature 245:49–52

Mungall JE (2002) Roasting the mantle: slab melting and the genesis of major Au and Au-rich Cu deposits. Geology 30:915–918

Pan GT, Wang PS, Xu YR, Jiao SP, Xiang TX (1990) Cenozoic tectonic evolution of Qinghai–Xizang Plateau. Geological Publishing House, Beijing, pp 1–190 (in Chinese with English abstract)

Pasteris JD (1996) Mount Pinatubo volcano and "negative" porphyry copper deposits. Geology 24:1075–1078

Pearce NJG, Perkins WT, Westgate JA, Corton MP, Jakson SE, Neal CR, Chenery SP (1997) A compilation of new and published major and trace element data for NIST SRM 610 and NIST 612 glass reference materials. Geostand Newsl 21:115–144

Ratschbacher L, Frisch W, Chen C, Pan G (1996) Cenozoic deformation, rotation, and stress patterns in eastern Tibet and western Sichuan, China. In: Yin A, Harrision TM (eds) The Tectonic evolution of Asia. Cambridge University Press, New York, pp 227–249

Rui ZY, Huang CK, Qi GM, Xu J, Zhang MT (1984) Porphyry copper (molybdenum) deposits in China. Geological Publishing House, Beijing, pp 1–350 (in Chinese)

Sengor AMC, Natalin BC (1996) Paleotectonics of Asia: fragments of a synthesis. In: Yin A, Harrison TM (eds) The tectonics of Asia. Cambridge University Press, New York, pp 486–640

Sillitoe RH (1972) A plate tectonic model for the origin of porphyry copper deposits. Econ Geol 67:184–197

Sillitoe RH, Camus F (eds) (1991) A special issue devoted to gold deposits in the Chilean Andes. Econ Geol 86:1153–1345

Sun WD, Li SG, Chen YD, Li YJ (2002) Timing of synorogenic granitoids in the South Qinling, central China: constraints on the evolution of the Qinling–Dabie orogenic belt. J Geol 110:457–468

Sun WD, Arculus RJ, Kamenetsky VS, Binns RA (2004) Release of gold-bearing fluids in convergent margin magmas prompted by magnetite crystallization. Nature 431:975–978

Tang RL, Luo HS (1995) The geology of Yulong porphyry copper (molybdenum) ore belt, Xizang (Tibet). Geological Publishing House, Beijing, pp 1–320 (in Chinese with English abstract)

Urich T, Guenther D, Heinrich CA (1999) Gold concentrations of magmatic brines and the metal budget of porphyry copper deposits. Nature 399:676–679

Wang E, Burchfiel BC (1997) Interpretation of Cenozoic tectonics in the right-lateral accommodation zone between the Ailao Shan shear zone and the eastern Himalayan xyntaxis. Int Geol Rev 39:191–219

Wang Z, Shentu BY, Ding JC, Yao P, Geng QR (1995) Granitoid and its mineralization in the eastern Tibet China. Publishing House of the Southwestern University of Communication, Chengdu, pp 1–150 (in Chinese with English abstract)

Wang JH, Yin A, Harrison TM, Grove M, Zhang YQ, Xie GH (2001) A tectonic model for Cenozoic igneous activities in the eastern Indo-Asian collision Zone. Earth Planet Sci Lett 188:123–133

Watson EB, Harrison TM (1983) Zircon saturation revisited; temperature and compositional effects in a variety of crustal magma types. Earth Planet Sci Lett 64:295–304

Yin A, Harrison T M (2000) Geological evolution of the Himalayan–Tibetan orogen. Annu Rev Earth Planet Sci 28:211–280

Zhang YQ, Xie YW, Qiu HN, Li XH, Chung SL (1998) Geochemical characteristics of the ore-bearing porphyries in the Yulong ore-belt. Earth Sci China Univ Geosci 23:560–597 (in Chinese with English abstract)

Zhang YQ, Xie YW, Li XH, Qiu HN, Zhao ZH, Liang HY, Chung SL (2000) Isotopic characteristics of shoshonitic rocks in eastern Qinghai–Tibet Plateau: petrogenesis and its tectonic implication. Sci China Ser D 30:494–498 (in Chinese with English abstract)